Inorganica Chimica Acta 367 (2011) 173–181

Contents lists available at ScienceDirect

Inorganica Chimica Acta

journal homepage: www.elsevier.com/locate/ica

Synthesis and photophysical studies of CdTe quantum dot-monosubstituted zinc phthalocyanine conjugates

Sarah D' Souza, Edith Antunes, Tebello Nyokong *

Department of Chemistry, Rhodes University, Grahamstown 6140, South Africa

ARTICLE INFO

Article history:
Received 26 March 2010
Received in revised form 25 November 2010
Accepted 10 December 2010
Available online 16 December 2010

Keywords:
Quantum dots
Aminophenoxy phthalocyanine
Fluorescence quantum yields
Förster resonance energy transfer

ABSTRACT

The linkage of unsymmetrically monosubstituted 4-aminophenoxy zinc phthalocyanine (ZnAPPc, **5**) to CdTe quantum dots capped with mercaptopropionic acid (MPA), L-cysteine (L-cys) or thioglycolic acid (TGA) has been achieved using the coupling agents ethyl-*N*(3-dimethylaminopropyl) carbodiimide and *N*-hydroxy succinimide, which facilitate formation of an amide bond to form the QD–ZnAPPc-linked conjugate. The formation of the amide bond was confirmed using Raman and IR spectroscopies. Atomic force microscopy (AFM) and UV–Vis spectroscopy were used further to characterise the conjugate. Förster resonance energy transfer (FRET) resulted in stimulated emission of ZnAPPc in both the linked (QD–ZnAPPc-linked) and mixed (QD:ZnAPPc-mixed) conjugates. The linked L-cys and TGA QDs conjugates (QD–ZnAPPc-linked) gave the largest FRET efficiencies hence showing the advantages of covalent linking. Fluorescence quantum yields of QDs were decreased in QD:ZnAPPc-mixed and QD:ZnAPPc-linked.

1. Introduction

Metallophthalocyanines (MPcs) have potential for application in many areas such as in electrophotography, chemical sensors, liquid crystals, non-linear optics, optical data storage and as carrier generation materials in near-IR devices [1–5]. Phthalocyanines have also been used as photosensitisers in photodynamic therapy (PDT), due to their strong absorption in the red (Q-band) which overlaps with the region of maximum light penetration in tissues [6].

MPcs possess high thermal stability due to both the interlinking nitrogen atoms [7] and an extended π electron conjugated system [8]. In recent years, there has been increasing interest in low symmetry MPc derivatives, which can provide the unique properties required for use in specific applications. The design of these low symmetry compounds has become the focus of intense interest amongst many phthalocyanine researchers [9]. However synthesis of low symmetry MPc compounds through statistical condensation results in a wide variety of derivatives which require lengthy separation. In this work we report on a new zinc phthalocyanine monosubstituted with a 4-aminophenoxy group (ZnAPPc, compound **5**, Scheme 1). The use of aminophenoxy as a substituent in MPc compounds has been reported [10], but their use in low symmetry compounds is reported here for the first time. The new molecule is covalently linked to thiol capped CdTe quantum dots, Scheme 2.

Quantum dots (QDs) are semiconducting nanoparticles, approximately 2-10 nm in diameter (10–50 atoms) [11], and their unique physical properties can be tuned by changing their size [12]. QDs have high photostability, broad absorption spectra and a narrow emission range, such that light of the correct wavelength causes simultaneous excitation (fluorescence) of various sizes of quantum dots [12,13].

Energy transfer from QDs to different phthalocyanine photosensitizers has been demonstrated in a number of studies [14–17] where the two components are mixed together, through a process called Förster resonance energy transfer (FRET). In most reported FRET studies, quantum dots were not covalently bound to phthalocyanines, but were mixed. Covalent linking of QDs to the Pc ring has not received much attention, apart from a report on the conjugates of SiPc with CdSe core QDs through axial ligation [18] and our recent reports of covalent linking of QDs to symmetrically substituted Zn (ZnTAPc) and In (InTAPc) tetraamino phthalocyanine [19,20]. However, in the case of ZnTAPc and InTAPc the linking point of the QDs to Pcs could be through some or all of the four amino groups. In the current work only one amino group is available, thus this should result in a more defined covalent link between QDs and ZnAPPc. The linking agents *N*-ethyl-*N*(3-dimethylaminopropyl) carbodiimide (EDC) and *N*-hydroxy succinimide (NHS) were employed for catalysing the formation of the amide bond between the carboxylic acid of QDs and the amino group of monosubstituted 4-aminophenoxy zinc phthanocyanine (ZnAPPc, **5**). The use of two coupling agents is due to the fact that Jiang et al. [21] have estimated that when using a mixture of EDC and NHS, about 60% of carboxylic acid groups are NHS-activated and

* Corresponding author. Tel.: +27 46 6038260; fax: +27 46 6225109.
E-mail address: t.nyokong@ru.ac.za (T. Nyokong).

0020-1693/$ - see front matter © 2010 Elsevier B.V. All rights reserved.
doi:10.1016/j.ica.2010.12.027

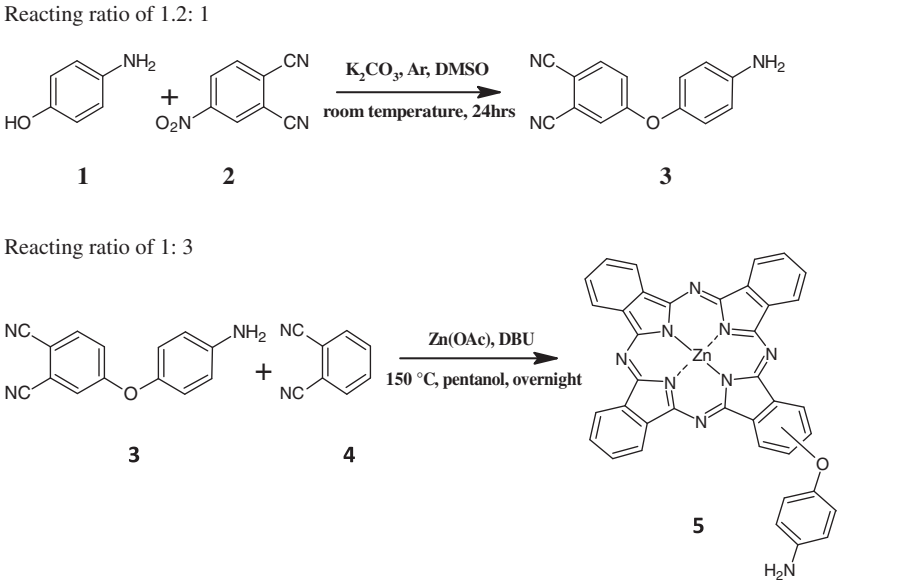

Scheme 1. Synthesis of ZnAPPc (**5**) derivative.

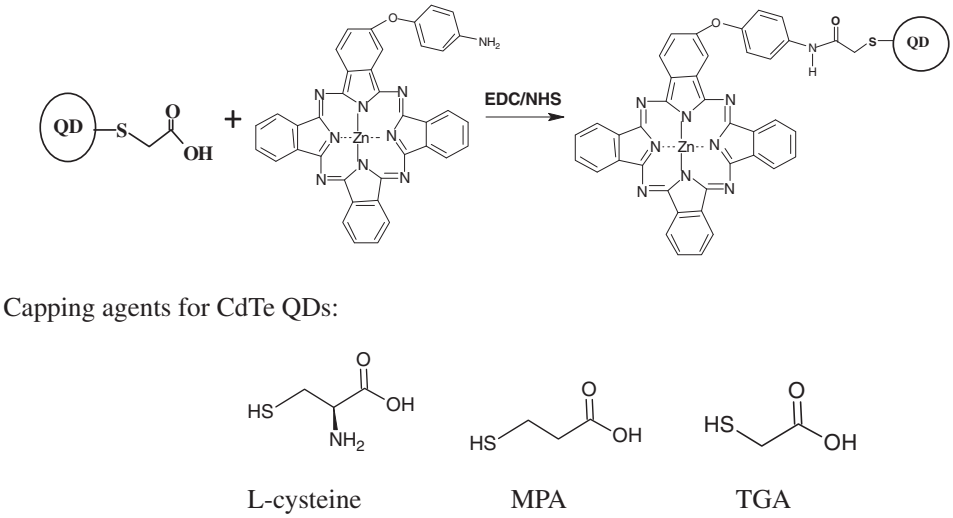

Scheme 2. Representation of the link formation of QDs to compound **5** and molecular structure of the capping agents for QDs: L-cysteine, MPA (mercaptopropionic acid) and thioglycolic acid (TGA).

30% EDC-activated leaving only 10% not activated. There is less activation if either EDC or NHS is employed separately.

2. Experimental

2.1. Materials

Tellurium powder (200 mesh), L-cysteine, 3-mercaptopropionic acid (MPA), thioglycolic acid (TGA), dimethylsulphoxide (DMSO) and anhydrous potassium carbonate were obtained from SAARCHEM. Ultra pure water was obtained from a Milli-Q Water System (Millipore Corp., Bedford, MA, USA). Trifluoroacetic acid (TFA), 1,8-diazabicyclo[5.4.0]undec-7-ene (DBU), *N*-ethyl-*N*(3-dimethylaminopropyl) carbodiimide (EDC), *N*-hydroxy succinimide (NHS), aminophenol and 4-nitrophthalonitrile were purchased from Fluka. Zinc acetate dihydrate was obtained from British Drug House (BDH) Chemicals. DMSO-d_6 was obtained from Aldrich. C_{18} Phenomenex reverse phase C_{18} Sep-Pak columns and sephadex G25 column were employed for chromatographic separations. The rest of the reagents were obtained from commercial supplies and used as received.

2.2. Equipment

Fluorescence emission and excitation spectra were recorded on a Varian Eclipse spectrofluorimeter. Ground-state electronic absorption spectra were recorded on a Varian Cary 500 UV–Vis–NIR spectrophotometer. The mass spectra were acquired on a Bruker Daltonics (Bremen, Germany) Autoflex III MALDITOF mass spectrometer. ^{1}H NMR spectra were obtained using a Bruker AMX 400 MHz and a Bruker Avance II+ 600 MHz NMR spectrometer. X-ray powder diffraction patterns were recorded on a Bruker D8 Discover equipped with a proportional counter, using Cu Kα radiation (λ = 1.5405 Å, nickel filter). Data were collected in the range from $2\theta = 5°$ to 60°, scanning at $1° \text{ min}^{-1}$ with a filter time-constant of 2.5 s per step and a slit width of 6.0 mm. Samples

were placed on a zero background silicon wafer slide. The X-ray diffraction (XRD) data were treated using Eva (evaluation curve fitting) software. Baseline correction was performed on each diffraction pattern by subtracting a spline fitted to the curved background and the full-width at half-maximum values used in this study were obtained from the fitted curves. Elemental analysis was carried out using a VARIO ELEMENTAR EL III CHNS instrument. FT-IR spectra (KBr pellets) were recorded on a Perkin–Elmer spectrum 2000 FT-IR spectrometer. Raman spectral data were collected with Bruker RAM II spectrometer (equipped with a 1064 nm Nd:YAG laser and a liquid nitrogen cooled germanium detector). Liquid samples in DMSO:H_2O as the solvent were employed. Atomic force microscopy (AFM) images were recorded in the non-contact mode in air with a CP-11 Scanning Probe Microscope from Veeco Instruments (Carl Zeiss, South Africa) at a scan rate of 1 Hz. Samples for AFM were prepared by spin coating samples of QDs in NaOH or DMSO:-water (10:1) solvent mixture (the latter in the absence or presence of compound **5**).

Fluorescence lifetimes were measured using a time correlated single photon counting setup (TCSPC) (FluoTime 200, Picoquant GmbH). The excitation sources were a light emitting diode (LED, PLS-500, 497 nm, 10 MHz repetition rate, Picoquant GmbH) with a linear polariser and a diode laser (LDH-P-C-485, 480 nm, 10 MHz repetition rate, Picoquant GmbH). The response function of the system, which was measured with a scattering Ludox solution (DuPont), had a full width at half-maximum (FWHM) of about 950 ps. The ratio of stop to start pulses was kept low (below 0.05) to ensure good statistics. All luminescence decay curves were measured at the maximum of the emission peak. The data were analysed with the program FluoFit (Picoquant GmbH). The support plane approach was used to estimate the errors of the decay times.

2.3. Fluorescence studies

2.3.1. Fluorescence quantum yields

Fluorescence quantum yields (Φ_F) of the QDs or compound **5** were determined by the comparative method [22] (Eq. (1)),

$$\Phi_F = \Phi_{F(Std)} \frac{F \cdot A_{Std} \cdot n^2}{F_{Std} \cdot A \cdot n^2_{Std}} \quad (1)$$

where F and F_{Std} are the areas under the fluorescence curves of the QDs (or compound **5**) and the reference, respectively. A and A_{Std} are the absorbances of the sample and reference at the excitation wavelength respectively, and n and n_{Std} are the refractive indices of solvents used for the sample and reference, respectively. ZnPc in DMSO was employed as a standard, $\Phi_F = 0.2$ [23] for compound **5**, whilst rhodamine 6G in ethanol with $\Phi_F = 0.94$ was employed as the standard for the quantum dots [24,25]. Both the sample and reference were excited at the same relevant wavelength (610 nm for compound **5** and 500 nm for QDs). The absorbance of the ZnPc standard (or compound **5**) or of QDs at the excitation wavelength ranged between 0.04 and 0.05. The determined fluorescence quantum yield values of the QDs were employed in determining their fluorescence quantum yields in the mixture with compound **5** ($\Phi^{Mix}_{F(QD)}$) or linked $\Phi^{linked}_{F(QD)}$ using Eq. (2):

$$\Phi^{Mix}_{F(QD)} = \Phi_{F(QD)} \frac{F^{Mix}_{QD}}{F_{QD}} \quad (2a)$$

$$\Phi^{linked}_{F(QD)} = \Phi_{F(QD)} \frac{F^{linked}_{QD}}{F_{QD}} \quad (2b)$$

where Φ_F(QD) is the fluorescence quantum yield of the QDs alone and was used as standard, F^{Mix}_{QD} (or F^{linked}_{QD}) is the fluorescence intensity of QDs, in the mixture (or linked) with compound **5** when excited at the excitation wavelength of the QDs (500 nm) and F_{QD} is the fluorescence intensity of the QD alone at the same excitation wavelength.

2.3.2. FRET parameters

FRET efficiency (*Eff*) is determined experimentally from the fluorescence quantum yields of the donor in the absence ($\Phi_{F(QD)}$) and presence (Φ^{Mix}_{QD}) of the acceptor using Eq. (3) [25–27]:

$$Eff = 1 - \frac{(\Phi^{Mix}_{F(QD)})}{(\Phi_{F(QD)})} \quad (3)$$

FRET efficiency (*Eff*) is related to r (Å) by Eq. (4) [25,28]:

$$Eff = \frac{R_0^6}{R_0^6 + r^6} \quad (4)$$

where r is the centre-to-centre separation distance (in Å) between donor and acceptor, R_0 (the Förster distance, Å) is the critical distance between the donor and the acceptor molecules at which the efficiency of energy transfer is 50% and depends on the quantum yield of the donor Eq. (5) [25,28]:

$$R_0^6 = 8.8 \times 10^{23} \kappa^2 n^{-4} \Phi_{F(QD)} J \quad (5)$$

where κ^2 is the dipole orientation factor, n the refractive index of the medium, Φ_F the fluorescence quantum yield of the donor in the absence of the acceptor, and J is the Förster overlap integral, defined by Eq. (6):

$$J = \Phi_{QD}(\lambda) \varepsilon_{ZnPc}(\lambda) \lambda^4 \delta\lambda \quad (6)$$

where f_{QD} is the normalised QD emission spectrum and ε_{ZnPc} is the molar extinction coefficient of ZnPc derivatives, λ is the wavelength of the acceptor, at the Q-band. In this case, it is assumed that κ^2 is 2/3 for mixed QDs with compound **5**; such assumption is often made for donor–acceptor pairs in a liquid medium, since their dipole moments are considered to be isotropically oriented during the excited state lifetimes. Although electrostatic interactions are anticipated between QDs and the sterically demanding phthalocyanines in mixed QDs, the exact orientation of the ZnPc derivative with regard to the QD is not known with certainty. Various conformations can be attained by the phthalocyanine compound on the surface of QDs when the two are mixed. For the perpendicular orientation of the ZnPc derivative on the QD some degree of movement of the donor/acceptor species is expected. As a result the isotropic dynamical average ($\kappa^2 = 2/3$) is more appropriate than the static isotropic average ($\kappa^2 = 0.476$) because the donor–acceptor pair is not rigid. The $\kappa^2 = 2/3$ was also employed for the linked QDs–ZnAPPc. FRET parameters were computed using the program PHOTOCHEMCAD [29].

2.4. Synthesis of CdTe quantum dots

The preparation of thiol capped QD was via a modified method adopted from literature [15,30]. Briefly, 2.35 mmol of $CdCl_2 \cdot H_2O$ was dissolved in 125 ml of water and 5.7 mmol of the respective carboxylic acid thiol {L-cysteine (L-cys), 3-mercaptopropionic acid (MPA) and thioglycolic acid (TGA), Scheme 2} was added under stirring. The solution was adjusted to a pH between 11 and 12 with 1 M NaOH. Nitrogen gas was bubbled through the solution for about 1 h. The aqueous solution was reacted with H_2Te gas, which was generated by the reaction of $NaBH_4$ with Te powder in the presence of 0.5 M H_2SO_4 under a flow of nitrogen gas. A change of colour of the solution containing $CdCl_2$ and the thiol was observed on addition of H_2Te gas. The solution was then refluxed under air at 100 °C for different times to control the size of the CdTe QDs. On cooling, the QDs were precipitated out from solution using excess ethanol, the solutions were then centrifuged to harvest the

QDs. Sizes (D) of the synthesized QDs were estimated using the polynomial fitting function [31] Eq. (7),

$$D = (9.8127 \times 10^{-7})\lambda^3 - (1.7147 \times 10^{-3})\lambda^2 + (1.0064)\lambda - (194.84) \quad (7)$$

where λ is the absorption maxima of the QDs. The fitting function is not valid for sizes of quantum dots outside the size range 1–9 nm [31]. The size was also determined using XRD. The particle diameter, d, for XRD data was determined using the Scherrer Eq. (8),

$$d(\text{Å}) = \frac{k\lambda}{\beta\cos\theta}. \quad (8)$$

where k is an empirical constant equal to 0.9, λ is the wavelength of the X-ray source (1.5405 Å), β is the full width at half maximum of the diffraction peak, and θ is the angular position of the peak.

2.5. Synthesis of monosubstituted 4-aminophenoxy zinc phthalocyanine (**5**)

2.5.1. 4-Aminophenoxyphthalonitrile (**3**, Scheme 1)

To a suspension of 4-aminophenol {(**1**) 0.76 g, 6.94 mmol}, 4-nitrophthalonitrile {(**2**) 1 g, 5.78 mmol} in 25 mL of dry DMSO was added anhydrous K_2CO_3 (1.64 g, 11.56 mmol). The mixture was left to reflux under argon overnight with stirring. A further 0.8 g (5.48 mmol) of K_2CO_3 was added after 24 h to the suspension. After 48 h, the resulting product was poured into 1 M HCl (260 mL), forming a precipitate that was recrystallized from methanol/water (1:1) to yield a dark brown product. Yield: 0.613 g (45.1%). ^{1}H NMR (DMSO-d_6): δ, ppm 8.25–8.31 (1H, m, Ar–H), 7.68–7.73 (1H, m, Ar–H), 8.0–8.7 (1H, m, Ar–H), 7.13–7.48 (4H, m, Ar–H).

2.5.2. Monosubstituted 4-aminophenoxy zinc phthalocyanine (ZnAPPc, **5**)

To a suspension of 1,2 dicyanobenzene {(**4**) 0.11 g, 0.84 mmol}, 4-aminophenoxyphthalonitrile {(**3**) 0.066 g,0.28 mmol} and zinc acetate (0.0671 g, 0.306 mmol) in 5 mL of pentanol, 2 mL of DBU was added. The mixture was left to reflux under argon overnight with stirring. The resulting product was cooled before the addition of methanol, precipitating compound **5** from the solution. The precipitate was collected using centrifugation and further purified by centrifuging with a 1:1 mixture of chloroform and dichloromethane. This choloroform/dichloromethane mixture was then removed using a rotary evaporation. The product was further purified using a Phenomenex C_{18} Sep-Pak column with 0.05% TFA in methanol as the solvent. Yield: 0.055 g (29%). UV–Vis (DMSO), λ_{max} (nm) (log ε): 673 (4.6), 608 (3.8), 346 (4.1). IR [(KBr) ν_{max}/cm^{-1}]: 3414 (NH_2), 2924 (C=C), 1647–1596 (NH bend), 1484 (C=C), 1327 (C–O–C), 1114–1060 (CN), 731 (Zn–N). ^{1}H NMR (DMSO-d_6): δ, ppm 9.68–9.71 (2H, br s, Ar–H), 9.43–9.45 (6H, m, Pc–H), 8.25–8.29 (6H, m, Pc–H), 7.9–7.96 (3H, m, Pc–H), 7.82–7.84 (4H, m, Ph–H). *Anal.* Calc. for $C_{38}H_{21}N_9OZn$: C, 66.57; H, 3.09; N, 18.41. Found: C, 67.32; H, 3.29; N, 18.10%. MALDI-TOF MS m/z calc. 685.04 amu, found 684.14 amu $(M)^+$.

2.5.3. Synthesis of linked QDs ZnAPPc conjugate

For the formation of the amide linked QD–ZnAPPc, a mixture containing 2 mM NHS, 5 mM EDC, CdTe QDs (0.001 g/mL) and ZnAPPc (compound **5**, 1×10^{-4} M) in DMSO was allowed to react for 1 h. Experiments, where the ZnAPPc were mixed with QDs, without covalent linking, resulting in mixed QD:ZnAPPc were also performed, using the same ratio of QDs to compound **5** as was used for the formation of the linked conjugate. The linked QDs–ZnAPPc conjugate was purified by first washing with water to remove excess NHS, EDC and unlinked QDs (as the linked conjugates are not soluble in 100% water). The sample was then run through a Sephadex column to separate any residual impurities such as the unlinked ZnAPPc from the linked which elutes first whilst the remaining bands are discarded.

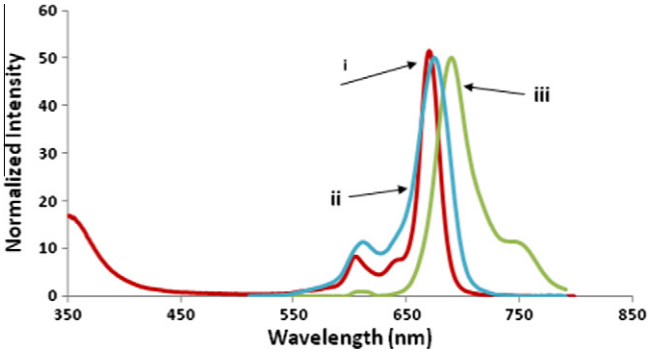

Fig. 1. Absorbance (i), excitation (ii) and emission (iii) spectra of compound **5** (ZnAPPc) in DMSO:water (10:1) solvent mixture (excitation wavelength = 671 nm), 5×10^{-4} M.

3. Results and discussion

3.1. Synthesis and characterisation

3.1.1. Monosubstituted 4-aminophenoxy zinc phthalocyanine (ZnAPPc, **5**)

The synthesis of the dinitrile precursor (**3**) was adapted from literature [32] for similar compounds with moderate yields. The synthetic procedure outlined in Scheme 1 shows the statistical condensation approach used for the synthesis of compound **5**. This method is based on the reaction of two differently substituted phthalonitriles in a ratio of 3:1. Following extensive purification, the target compound was obtained in low yields (29%), with the Q band at 673 nm in DMSO, Fig. 1. The elemental analyses and mass and ^{1}H NMR spectral data for compound **5** were consistent with its structure. Beer's law was observed for compound **5** for concentrations less than 5×10^{-5} M. The compound is unsymmetrically substituted and it would be expected that there is some Q band splitting due to loss of symmetry, however, this is not clear from the absorption spectra in Fig. 1. Fig. 1 shows broadening on the excitation spectrum when compared to the absorption spectrum, suggesting loss of symmetry on excitation. The loss of symmetry, due to unsymmetrical nature of the molecule, is even more evident in the fluorescence spectrum (Fig. 1(iii)). A Stokes shift of 15 nm was observed and is typical of MPc compounds [23].

3.1.2. Quantum dots

QDs grow through the Ostwald ripening process during the course of heating. As they grow, both the absorbance and the emission spectra shift to longer wavelengths. The QDs emission wavelengths chosen for FRET work are shown in Table 1.

Table 1
Emission spectral data and size determination of CdTe core QDs quantum dots using different methods. For the polynomial fitting water was employed as the solvent.

Thiol capping	λ (emission) (nm)	Size (nm)		FWHM[a]
		Polynomial (Eq. (7))	XRD	
MPA	621	3.5	3.9	60
TGA	614	3.2	3.4	59
L-cysteine	601	3.5	4.1	73

[a] FWHM = full width at half maximum.

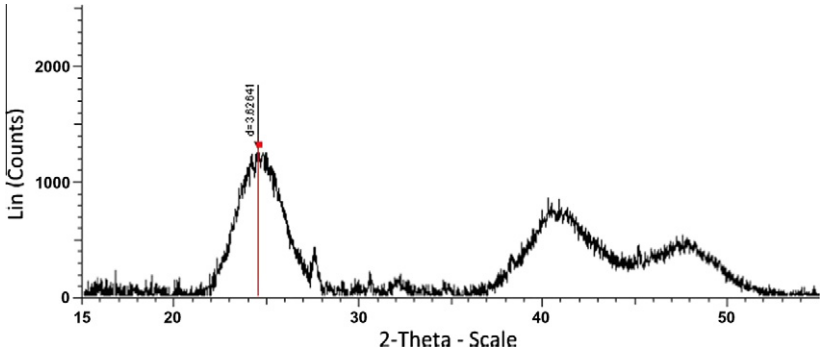

Fig. 2. XRD plot for CdTe–MPA capped QDs.

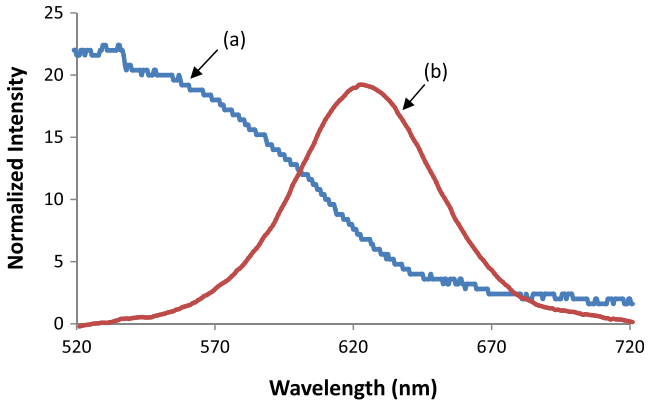

Fig. 3. Absorbance (a) and fluorescence (b) spectra of MPA coated CdTe in DMSO:water (9:1).

The X-ray diffraction pattern of CdTe MPA QDs employed in this work is shown in Fig. 2. Although the diffraction pattern is rather broad, it corresponds well with the three characteristic peaks for bulk CdTe structure. X-ray powder diffraction can provide important details about the crystal structure and properties of the QDs and so this technique was employed to determine the size of the CdTe QDs. According to the estimate obtained using Eq. (7), the size of the MPA coated CdTe core QDs chosen for this work is 3.5 nm whilst the XRD calculation gives the size to be 3.9 nm (Table 1) using Fig. 2. The sizes for CdTe TGA QDs and CdTe L-cys QDs are also slightly higher when using XRD as opposed to the polynomial. Since the polynomial used is only an estimate, the sizes determined by XRD will be employed in this work. Fig. 3 shows the absorption and fluorescence emission spectra of the synthesized QDs in DMSO:water (9:1), using CdTe MPA QDs as an example. This solvent mixture allows for solubilisation of the quantum dots whilst maintaining the phthalocyanine in its monomeric form, hence QDs alone were also studied in this mixture. The full width at half maximum (FWHM, Table 1) is an indication of the quality of the QDs and should be ~70 nm or less. The synthesized QDs show the FWHM to be in this region.

CdTe QDs capped with thiols are known to aggregate in acidic conditions due to detachment of surface ligands [33]. Aggregation of QDs results in red shifting in the emission spectra accompanied by broadening [34]. Solvents also have an effect on the aggregation nature of CdTe QDs [34]. There was no change in FWHM of the QDs recorded from direct synthesis conditions in NaOH or when recorded using DMSO:water mixture. The emission spectra shifted from 627 nm in 0.1 M NaOH to 622 nm in DMSO:water, hence showing red shifting in NaOH.

Atomic force microscopy data (Fig. 4) provided the information about surface morphology of CdTe QDs on a cross section of the glass surface coating from a 0.1 M NaOH, DMSO:water solvent mixture and in the presence of compound **5**. In 0.1 M NaOH solution only, the CdTe QDs show a size distribution from 4 to 27 nm (Fig. 4E) however populations with size distributions from 12 nm and below in the section analysed occurred more frequently suggesting that CdTe QDs are not totally monodisperse even in basic media. In DMSO:water the QDs show a size distribution of from 2 to up to 60 nm (Fig. 4D) which is a very wide distribution, suggesting that aggregation tendencies are worsened in this solvent system, and also showing the reported solvent dependency [34]. The same aggregation behaviour was observed in the presence of compound **5**. However, in the presence of compound **5**, the AFM histograms showed that clusters of a size distribution of 11 nm and less were more predominant indicating that the more aggregated clusters occur less frequently Fig. 4F. The AFM images in the presence of compound **5**, Fig. 4C, shows more enhanced clusters as opposed to smaller dots observed for QDs alone in DMSO:water, Fig. 4A.

3.1.3. Linked QDs–ZnAPPc

The capping agent located on the surface of CdTe core QDs were linked to ZnAPPc (compound **5**) by coupling the carboxylic group of the capping agent to the amino group on **5** using EDC/NHS mixture as a linking agent. The resulting conjugate is represented as QD–ZnAPPc-linked. EDC and NHS were employed as linking agents, catalysing the formation of the amide bond between the carboxylic acid of QDs and the amine group of ZnAPPc.

Raman spectra were collected in order to characterise the new compound and conjugates, Fig. 5. The main difference between the linked (QD–ZnAPPc-linked, Fig. 5a) and mixed (QD:ZnAPPc-mixed, Fig. 5b) conjugates was the position of the main peaks attributed to the phthalocyanine structure (Fig. 5c) at 2916 and 3004 cm^{-1}. For the QD:ZnAPPc-mixed, there was no peak in this region as was the case with QDs alone. The peak for the QD–ZnAPPc-linked conjugates was shifted from 2916 cm^{-1} (for ZnAPPc alone) to 2923 cm^{-1}. The shifts (or absence) of the peaks in this region confirm the formation of QD–ZnAPPc-linked conjugate due to changes in the molecular structure as a result of bond formation between the QDs and ZnAPPc.

In the IR spectrum of the linked QD–ZnAPPc, Fig. 6a, there was an indication of amide bond formation by the presence of a band characteristic of the amides at 1664 cm^{-1} whilst it was not observed in the mixture of QDs with ZnAPPc, Fig. 6b. The differences between the mixed and the linked confirm the linking.

Absorption spectra were used for further characterisation of the mixed and linked species in the DMSO:water solvent mixture (Fig. 7). Interestingly there was a shift in the Q band from 673 nm (of ZnAPPc alone) to 678 nm upon formation of the QD–ZnAPPc-linked, showing changes in the environment. The mixed Q band gave a Q band very close to that of ZnAPPc alone at 674 nm. The spectra of the QD–ZnAPPc-linked does not show

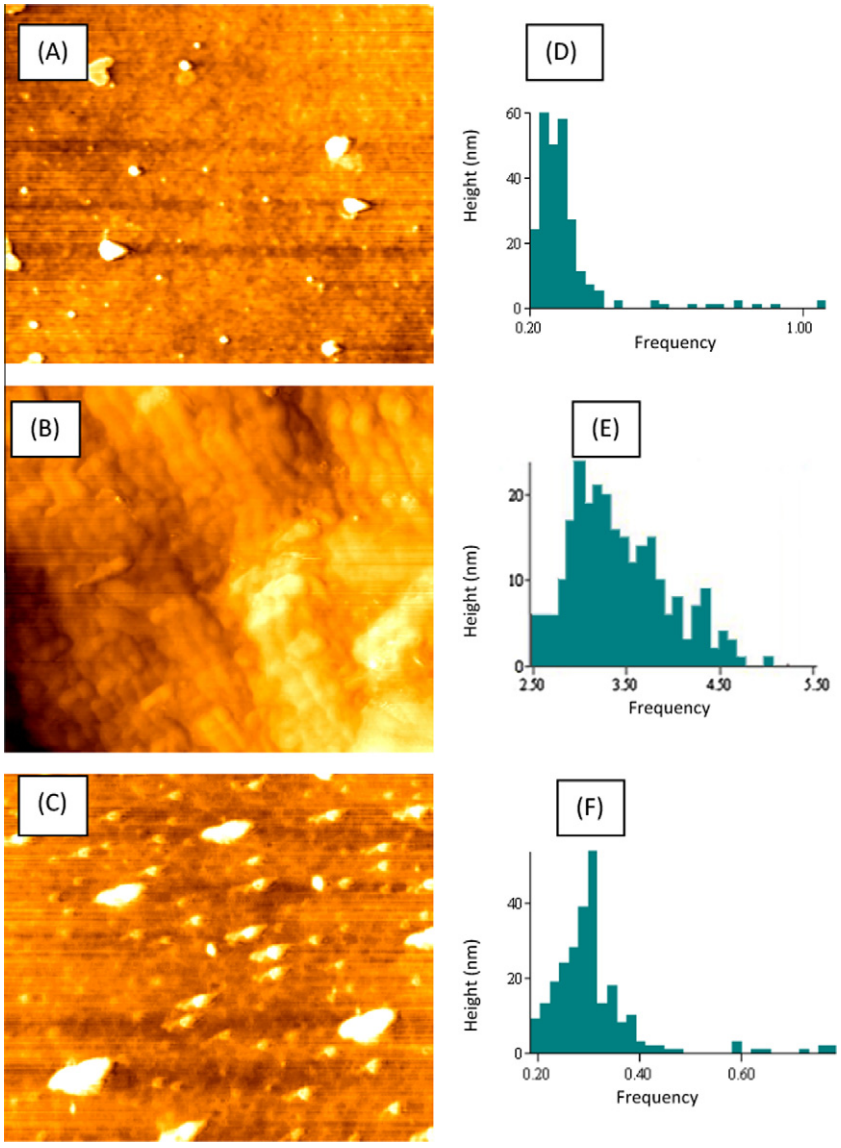

Fig. 4. AFM images of MPA CdTe QDs deposited on a glass surface from (A) 0.1 M DMSO:water (9:1), (B) 0.1 M NaOH and (C) QDs and ZnAPPc in DMSO:water (9:1). Corresponding histograms (D, E and F).

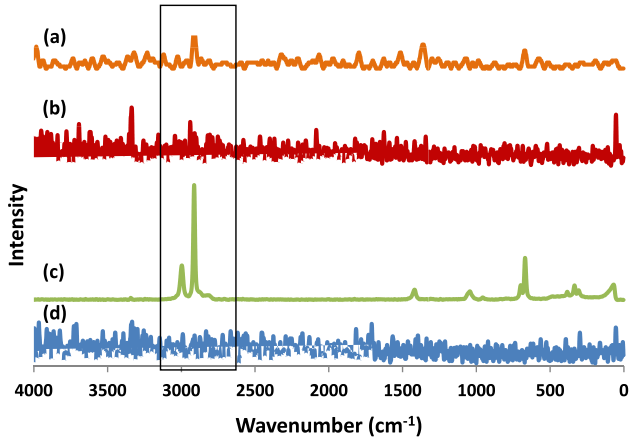

Fig. 5. Raman spectra of (a) ZnAPPc–CdTe–MPA QD linked, (b) ZnAPPc–CdTe–MPA QD mixed, (c) ZnAPPc alone and (d) CdTe MPA QDs alone in DMSO:water.

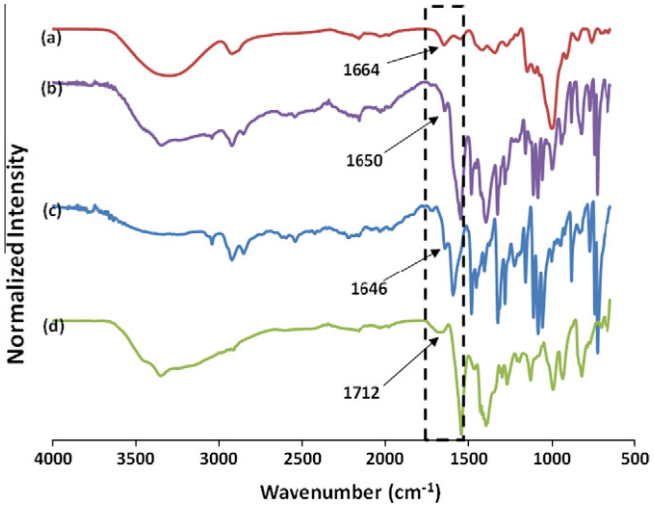

Fig. 6. IR spectra of (a) ZnAPPc – CdTe–MPA linked, (b) ZnAPPc + CdTe–MPA mixed, (c) ZnAPPc (compound **5**) and (d) MPA capped QDs.

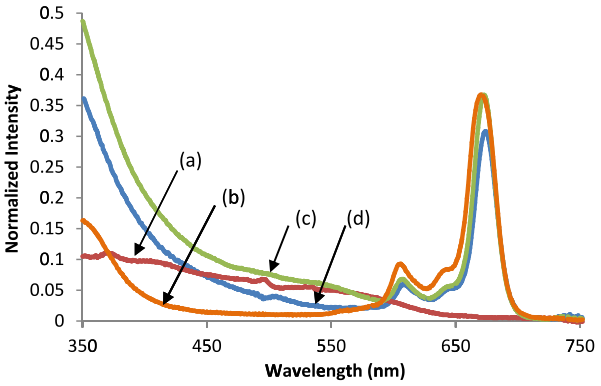

Fig. 7. Ground state electronic absorption spectra and Q band position of (a) CdTe MPA QDs alone, (b) ZnAPPc alone (673 nm), (c) QD:ZnAPPc-mixed (674 nm) and (d) QD–ZnAPPc-linked (678 nm) in 9:1 *v/v* DMSO:water solution.

Table 2
Fluorescence quantum yield parameters for ZnAPPc:CdTe core QD interaction in DMSO:water (9:1) mixture for both the linked and mixed conjugates.

Thiol capping[a]	$\Phi_{F(QD)}$	$\Phi^{Mix}_{F(QD)}$	$\Phi^{Linked}_{F(QD)}$	Refs.
MPA (3.9)	0.57	0.21	0.04	This work
TGA (3.4)	0.57	0.48	0.03	This work
LCys (4.1)	0.04	0.03	0.004	This work
MPA (3.7)	0.59	–	–	[15][b]
TGA (3.6)	0.62	–	–	[15]
LCys (3.5)	0.09	–	–	[15]

[a] QD size in brackets.
[b] Data in pH 7.4 buffer.

aggregation. Aggregation in MPc compounds is characterised by the formation of a blue shifted band due to the aggregate. This is not observed in Fig. 7. Small shifts in phthalocyanine spectra may be attributed to changes in the environment such as axial ligation. This difference in spectra between the linked and mixed is an indirect way of confirming the linkage. There was an increase in absorption in the 500 nm region for QD–ZnAPPc-linked and QD:ZnAPPc-mixed due to the presence of QDs (using MPA capped QDs as an example). The QD–ZnAPPc-linked shows a lower absorption in the 500 nm region than QD:ZnAPPc-mixed, due to different amounts of QDs in the two.

3.2. Fluorescence quantum yields

The fluorescence quantum yield (Φ_F) value for compound **5** was calculated to be 0.33. This value is within the range for MPc compounds [23]. Fluorescence quantum yield (Φ_F) values for the CdTe core QDs in DMSO:H_2O (9:1) are listed in Table 2. The QDs show slightly lower quantum yields compared to the values obtained in pH 7.4 buffer for similar sized QDs [15], Table 2. When QDs were mixed with compound **5**, the $\Phi^{Mix}_{F(QD)}$ were even lower due to the known quenching effects of MPc compounds on QDs [15]. This is a regular occurrence for QDs in the presence of phthalocyanine units [15] and the quenching has been attributed to the transfer of energy from donor QDs to phthalocyanine acceptor molecules. This results in a lowering of QD fluorescence intensity, in either a QD:ZnAPPc-mixed or QD–ZnAPPc-linked species, and therefore a reduction in fluorescence quantum yields of the QDs. Non-radiative (NR) decay processes may also be used to account for the decline in Φ_F values.

3.3. Förster resonance energy transer (FRET)

FRET is a photophysical process through which an electronically excited fluorescent donor molecule (QDs in this case) transfers its

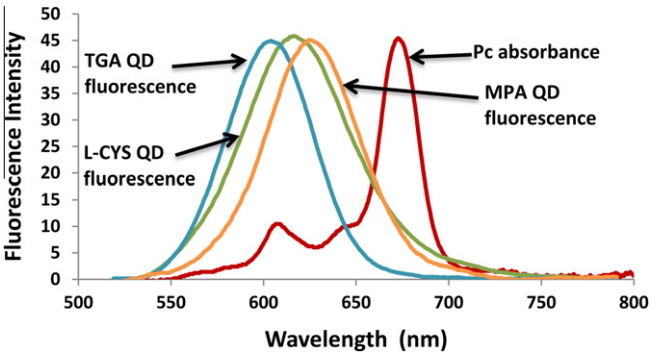

Fig. 8. Electronic spectrum showing the overlap between the absorption spectra of the ZnAPPc and the photoemission spectra of the respective QDs. Solvent: water.

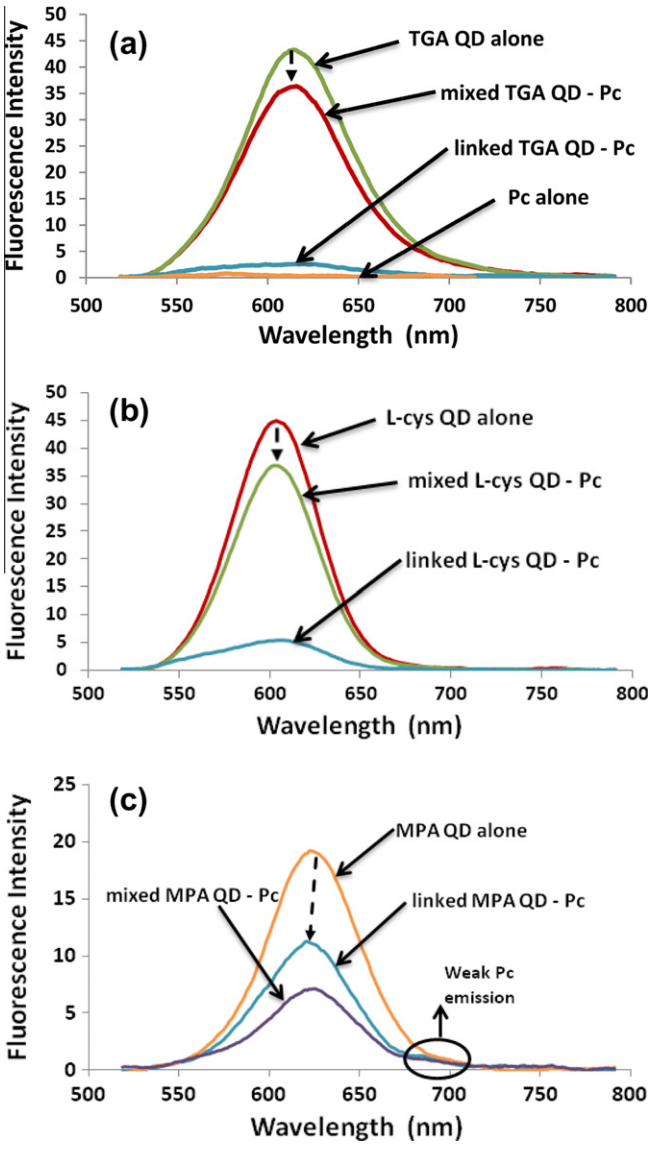

Fig. 9. Emission of QDs alone, ZnAPPc, QDs in the mixture with the ZnAPPc or ZnAPPc linked to QDs. (a) TGA, (b) L-cys and (c) MPA capped QDs. ($\lambda_{excitation}$ = 500 nm, in (9:1) DMSO:water solvent mixture).

excitation energy to an acceptor molecule (compound **5**) non-radiatively such that the acceptor is raised to a higher energy state. The acceptor may or may not be fluorescent.

In order for FRET to occur, there should be an overlap between the fluorescence spectra of QD with the absorption spectrum of ZnAPPc and this is observed in Fig. 8. On mixing solutions of ZnAPPc with QDs and monitoring the emission spectra of the QDs, a decrease in the fluorescence emission (on exciting at 500 nm where QDs absorb and compound **5** does not) of the latter was observed, Fig. 9. These changes are due to energy transfer from the QDs to ZnAPPc. There is no clear stimulated emission of ZnAPPc by TGA (Fig. 9a) and L-cys (Fig. 9b) capped QDs. For MPA capped QDs there is clear (but weak) stimulated emission at ~688 nm where ZnAPPc emits, for both mixed and linked QDs, Fig. 9c. It is important to note that the relative amounts of ZnAPPc and QDs will be different in the mixed and linked QD–ZnAPPc making comparison between the two difficult. The lack of clear stimulated emission for TGA capped QDS could be a result of less overlap between the emission spectrum of these QDs and the absorption spectrum of compound **5**. The overlap between absorption spectrum of compound **5** and emission spectrum of L-cys capped QDs is similar to that of MPA capped QDs, yet the latter show more stimulated emission, emphasising that the differences in the nature of capping agents can influence the quenching of the QDs emission.

Fig. 9 shows that for mixed QDs–ZnAPPc (where the ratio of QDs to ZnAPPc were kept the same for all the three types of QDs), the emission is quenched more for the MPA capped QDs compared to either L-cys or TGA capped QDs. In order study the differences between the quenching of the different QDs by ZnAPPc for mixed conjugates, time resolved fluorescence decay curves were recorded. A sample of the fluorescence decay curve is shown in Fig. 10. The fluorescence lifetimes are listed in Table 3. The presence of three lifetimes is common occurrence for QDs. Though there is lack of agreement in literature. However, the longer lifetime (τ_1 in Table 3) component is usually associated with the involvement of surface states in the carrier recombination process [35]. The shorter lifetime (τ_2 in Table 3) component may be attributed to the intrinsic recombination of initially populated core states [36–38] and the shortest lifetime (τ_3 in Table 3) is attributed to radiative depopulation due to band edge recombination at the surface [39]. Table 3 shows that MPA capped QDs gave the largest decreased (~26%) in the longest lifetime (τ_1) in the presence of compound **5** compared to the other two QDs hence there is more quenching of fluorescence in Fig. 9 for MPA capped QDs.

Table 3
Fluorescence lifetimes of MPA, L-cys and TGA capped QDs in the absence and presence of compound **5**.

Compound	τ_{F1} (ns)[a](±2.7)	τ_{F2} (ns) [a] (±1.2)	τ_{F3} (ns) [a] (±0.2)
MPA QDs alone	19.0 (0.23)	4.8 (0.33)	0.9 (0.45)
ZnAPPc–MPA QDs mixed	14.1 (0.25)	3.8 (0.37)	0.8 (0.38)
TGA QDs alone	23.6 (0.28)	4.4 (0.27)	0.8 (0.45)
ZnAPPc	18.5 (0.19)	2.9 (0.24)	0.4(0.57)
TGA QDs mixed			
L-cys alone	10.9 (0.03)	2.8 (0.21)	0.6 (0.76)
ZnAPPc–L-cys QDs linked	11.0 (0.03)	2.9 (0.21)	0.6 (0.76)

[a] Relative abundance in brackets.

3.4. Determination of FRET parameters

In FRET, the acceptor may or may not be fluorescent, hence FRET parameters are determined in section. FRET facilitates the non-radiative transfer of energy from the donor to the acceptor molecule. The efficiency of FRET is known to be dependent on a number of parameters such as the spectral overlap term (J) estimated by overlapping QD emission with the absorbance of ZnPc derivatives shown in Fig. 8. This extent of overlap has varied units and in this work the units used were in cm^6 [25]. The PhotochemCAD program gives J units as cm^6 following the use of ε_{ZnPc} in M^{-1} cm^{-1} and the wavelength λ in nm in Eq. (6). The J and R_0 values in this work were computed using PhotochemCAD [29] whilst the r values were calculated using Eq. (4) and are listed in Table 4.

J values are generally of the order of 10^{-14} cm^6 for porphyrin based molecules and the values obtained in this work were of the order 10^{-13} cm^6 in Table 4, thus confirming good spectral overlap, which is desirable since a greater value of J indicates good spectral overlap between the emission spectrum of the donor and the absorption spectrum of the acceptor giving an estimation of a good donor–acceptor oscillator match and hence a greater probability for FRET. This large J value would probably enhance the efficiency of energy transfer (FRET). The efficiency of FRET (*Eff*) values calculated using Eq. (3) from the QD to the ZnPc derivative are shown in Table 3.

The values of r were smaller than for R_0 for MPA capped QDs (for both the linked and mixed systems), showing that *Eff* will be greater than 50% as observed in Table 4. For TGA and L-cys capped QDs, $r < R_0$ for the QD–ZnAPPc-linked but not for QD:ZnAPPc-

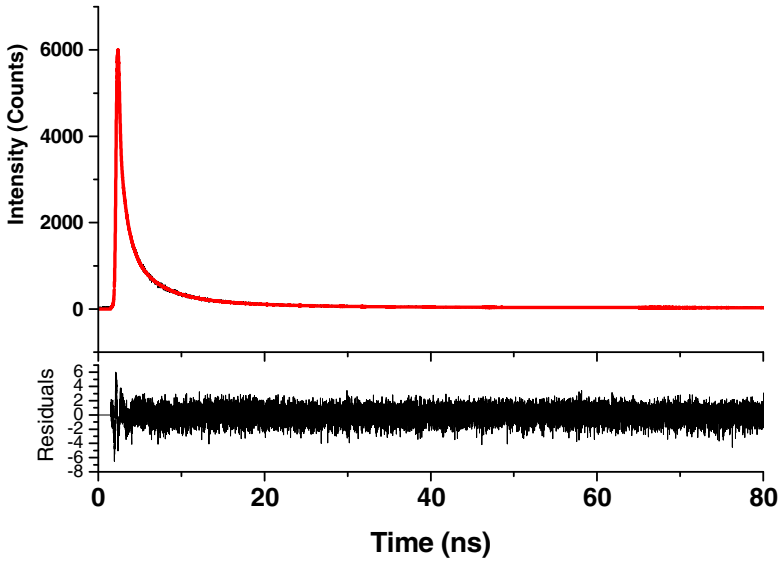

Fig. 10. Fluorescence decay curves of CdTe QDs (MPA capped) in the presence of ZnAPPc.

Table 4
Energy transfer parameters for ZnAPPc–CdTe: thiol QD interactions (in DMSO:H_2O (9:1) for linked and mixed conjugates).

Capping thiol	J ($\times 10^{-13}$ cm^6)	R_0 ($\times 10^{-10}$ m)	r ($\times 10^{-10}$ m)	*Eff*
ZnAPPc–CdTe–MPA QD mixed	1.36	46.52	42.57	0.63
ZnAPPc–CdTe–MPA QD linked	1.09	44.38	29.54	0.92
ZnAPPc–CdTe–TGA QD mixed	1.24	45.71	60.26	0.16
ZnAPPc–CdTe–TGA QD linked	0.84	42.53	26.04	0.95
ZnAPPc CdTe–L-cys QD mixed	0.78	26.46	34.46	0.17
ZnAPPc CdTe–L-cys QD linked	1.30	29.37	20.36	0.90

mixed. Higher *Eff* values were observed for the linked QDs–MTAPc when compared to the mixed QDs–MTAPc combinations, showing the advantages of covalent linking as expected. It has been observed before that MPA capped QDs show better *Eff* than their TGA counterparts for mixed MPc:QDs conjugates [15] and this is evident in Table 4 for the mixed conjugates. Also as seen in Fig. 9 clear stimulated emission for TGA and L-cys capped QDs in the presence of compound **5** was not observed, whereas MPA capped QDs stimulated emission of compound **5**. In addition, both the MPA and TGA capped QDs when linked to compound 5 show larger FRET efficiency compared to the L-cys capped QDs. It is feasible that the FRET efficiency observed for the linked species also comprises non-radiative processes, due to the strong involvement of surface states that may deactivate the QD fluorophores. Thus the data obtained may not be a true reflection of FRET alone.

4. Conclusions

The unsymmetrically monosubstituted 4-aminophenoxy zinc phthalocyanine (ZnAPPc) was successfully linked to the thiol capped quantum dots (QDs) and fully characterised. The linked ZnAPPc–QD conjugates showed higher FRET efficiencies for the L-cys and TGA QDs making them ideal photosensitizers for photodynamic therapy. The MPA linked ZnAPPc had a high fluorescence quantum yield which is advantageous in bioimaging.

Acknowledgements

This work was supported by the Department of Science and Technology (DST) and National Research Foundation (NRF), South Africa through DST/NRF South African Research Chairs Initiative for Professor of Medicinal Chemistry and Nanotechnology and Rhodes University, and by DST/Mintek Nanotechnology Innovation centre. Edith Antunes thanks CSIR/Swiss JRF of South Africa for Post-Doctoral funding. S.D. thanks the African Laser Centre for a bursary.

References

[1] P.J. Gregory, J. Porphyrins Phthalocyanines 4 (2000) 432.
[2] A.W. Snow, in: K.M. Kadish, K.M. Smith, R. Guilard (Eds.), Porphyrin Handbook, Phthalocyanine Properties and Materials, vol. 17, Academic Press, New York, 2003 (Chapter 109).
[3] E. Ben-Hur, W.S. Chan, in: K.M. Kadish, K.M. Smith, R. Guilard (Eds.), Porphyrin Handbook, Phthalocyanine Properties and Materials, vol. 19, Academic Press, New York, 2003 (Chapter 117).
[4] D. Dini, M. Hanack, in: K.M. Kadish, K.M. Smith, R. Guilard (Eds.), Porphyrin Handbook, Phthalocyanine Properties and Materials, vol. 17, Academic Press, New York, 2003 (Chapter 107).
[5] G. de la Torre, C.G. Claessens, T. Torres, Chem. Commun. (2007) 2000.
[6] M.C. DeRosa, R.J. Crutchley, Coord. Chem. Rev. 233 (2002) 351.
[7] T. Torres, J. Porphyrins Phthalocyanines 4 (2000) 325.
[8] T. Nyokong, H. Isago, J. Porphyrins Phthalocyanines 8 (2004) 1083.
[9] M.S. Rodriguez-Morgade, G. de La Torre, T. Torres, in: K.M. Kadish, K.M. Smith, R. Guilard (Eds.), Porphyrin Handbook, Phthalocyanine Properties and Materials, vol. 17, Academic Press, New York, 2003 (Chapter 107).
[10] S.E. Maree, T. Nyokong, J. Porphyrins Phthalocyanines 5 (2001) 782.
[11] T. Jamieson, R. Bakhshi, D. Petrova, R. Pocock, M. Imani, A.M. Seifalian, Biomaterials 28 (2007) 4717.
[12] J.H. Wang, H.Q. Wang, H.L. Zhang, X.Q. Li, X.F. Hua, Y.C. Cao, Z.L. Huang, Y.D. Zhao, Anal. Bioanal. Chem. 388 (2007) 969.
[13] C. Seydal, Science 300 (2003) 80.
[14] J. Ma, J.Y. Chen, M. Idowu, T. Nyokong, J. Phys. Chem. B 112 (2008) 4465.
[15] M. Idowu, J.Y. Chen, T. Nyokong, New J. Chem. 32 (2008) 290.
[16] S. Dayal, R. Krolicki, Y. Lou, X. Qiu, J.C. Berlin, M.E. Kenney, C. Burda, Appl. Phys. B 84 (2006) 309.
[17] S. Dayal, Y. Lou, A.C.S. Samia, J.C. Berlin, M.E. Kenney, C. Burda, J. Am. Chem. Soc. 128 (2006) 13974.
[18] S. Dayal, J. Li, Y.S. Li, H. Wu, A.C.S. Samia, M.E. Kenney, C. Burda, Photochem. Photobiol. 84 (2007) 243.
[19] J. Britton, E. Antunes, T. Nyokong, Inorg. Chem. Commun. 12 (2009) 828.
[20] J. Britton, E. Antunes, T. Nyokong, J. Photochem. Photobiol. A: Chem. 210 (2010) 1.
[21] L. Jiang, A. Glidle, A. Griffith, C.J. McNeil, J.M. Cooper, Bioelctrochem. Bioenerg. 42 (1997) 15.
[22] S. Fery-Forgues, D. Lavabre, J. Chem. Ed. 76 (1999) 1260.
[23] A. Ogunsipe, J.-Y. Chen, T. Nyokong, New J. Chem. 28 (2004) 822.
[24] R.F. Kubin, A.N. Fletcher, J. Lumin. 27 (1982) 455.
[25] J.R. Lakowicz, Principles of Fluorescence Spectroscopy, second ed., Kluwer Academic/Plenum Publishers, New York, 1999.
[26] J.S. Hsiao, B.P. Krueger, R.W. Wagner, T.E. Johnson, J.K. Delaney, D.C. Mauzerall, G.R. Fleming, J.S. Lindsey, D.F. Bocian, R.J. Donohoe, J. Am. Chem. Soc. 118 (2006) 11181.
[27] P. Jacques, A.M. Braun, Helv. Chim. Acta 64 (1981) 1800.
[28] T. Forster, Discuss. Faraday Soc. 27 (1959) 7.
[29] H. Du, R.A. Fuh, J. Li, L.A. Cockan, J.S. Linsey, Photochem. Photobiol. 68 (1998) 141.
[30] N. Gaponik, D.V. Talapin, A. Togach, K. Hoppe, E.V. Shevchenko, A. Eychmuller, H. Weller, J. Phys. Chem. 106 (2002) 7177.
[31] W.W. Yu, L. Qu, W. Guo, X. Peng, Chem. Mater. 15 (2003) 2854.
[32] D. Wöhrle, M. Eskes, K. Shigehara, A. Yamada, Synthesis (1993) 194.
[33] C. Bullen, P. Mulvaney, Langmuir 22 (2006) 3007.
[34] A. Mandal, N. Tamai, J. Phys. Chem. C 112 (2008) 8244.
[35] X. Wang, L. Qu, J. Zhang, X. Peng, M. Xiao, Nano Lett. 3 (2003) 1103.
[36] M. Lunz, A. Louise Bradley, J. Phys. Chem. C 113 (2009) 3084.
[37] J. Zhang, X. Wang, M. Xiao, Opt. Lett. 27 (2002) 1253.
[38] M.G. Bawendi, P.J. Carroll, W.L. Wilson, L.E. Bruce, J. Chem. Phys. 96 (1992) 946.
[39] M. Sanz, M.A. Correa-Duarte, L.M. Liz-Marzán, A. Douhal, J. Photochem. Photobiol. A: Chem. 196 (2008) 51.